

<b>Manuscript Number:</b>	GIGA-D-19-00237	
<b>Full Title:</b>	Genomic evidence of neo-sex chromosomes in the Eastern Yellow Robin	
<b>Article Type:</b>	Data Note	
<b>Funding Information:</b>	Australian Research Council (ARC) Discovery Project (DP180102359)	Prof Paul Sunnucks
	ARC Linkage Grant (LP0776322)	Prof Paul Sunnucks
<b>Abstract:</b>	<p>Background: Understanding sex-biased natural selection can be greatly enhanced by access to well-annotated chromosomes including ones inherited in sex-specific fashions. The Eastern Yellow Robin (EYR) is an endemic Australian songbird inferred to have experienced climate-driven sex-biased selection and is a prominent model for studying mitochondrial-nuclear interactions in the wild. However, the lack of an EYR reference genome containing both sex chromosomes (in birds, a female bearing Z and W chromosomes) is limiting current efforts to understand the mechanisms of these processes. Here, we assemble the genome for a female EYR and use low depth (10 ×) genome resequencing data from 19 individuals of known sex to identify chromosome fragments with sex-specific inheritance.</p> <p>Findings: MaSurCA hybrid assembly using Nanopore and Illumina reads generated a 1.22 Gb EYR genome in 20,702 scaffolds (94.2% BUSCO completeness). Scaffolds were tested for W-linked (female-only) inheritance using a k-mer approach, and for Z-linked inheritance using median read-depth test in male and female reads (read-depths must indicate haploid female and diploid male representation). This resulted in 2,372 W-linked scaffolds (total length: 97,872,282 bp, N50: 81,931 bp) and 586 Z-linked scaffolds (total length: 121,817,358 bp, N50: 551,641 bp). Anchoring of the sex-linked EYR scaffolds to the reference genome of a female Zebra Finch revealed two categories of sex-linked genome region. First, 653 W-linked scaffolds (25.7 Mb) were anchored to the W sex chromosome and 215 Z-linked scaffolds (74.4 Mb) to the Z. Second, 1138 W-linked scaffolds (70.9 Mb), and 179 Z-linked scaffolds (51.0 Mb), were anchored to a large section (coordinates ~5 to ~60 Mb) of Zebra Finch chromosome 1A. The first ~5 Mb and last ~14 Mb of the reference chromosome 1A had only autosomally-behaving EYR scaffolds mapping to them.</p> <p>Conclusions: We report a female (W-chromosome containing) EYR genome and provide genomic evidence for a neo-sex (neo-W and neo-Z) chromosome system in EYR, involving most of a large chromosome (1A) previously only reported to be autosomal in passerines.</p>	
<b>Corresponding Author:</b>	Han Ming Gan AUSTRALIA	
<b>Corresponding Author Secondary Information:</b>		
<b>Corresponding Author's Institution:</b>		
<b>Corresponding Author's Secondary Institution:</b>		
<b>First Author:</b>	Han Ming Gan	
<b>First Author Secondary Information:</b>		
<b>Order of Authors:</b>	Han Ming Gan	
	Stephanie Falk	
	Hernán E. Morales	

	Christopher M. Austin
	Paul Sunnucks
	Alexandra Pavlova
<b>Order of Authors Secondary Information:</b>	
<b>Additional Information:</b>	
<b>Question</b>	<b>Response</b>
Are you submitting this manuscript to a special series or article collection?	No
<p><b>Experimental design and statistics</b></p> <p>Full details of the experimental design and statistical methods used should be given in the Methods section, as detailed in our <a href="#">Minimum Standards Reporting Checklist</a>. Information essential to interpreting the data presented should be made available in the figure legends.</p> <p>Have you included all the information requested in your manuscript?</p>	Yes
<p><b>Resources</b></p> <p>A description of all resources used, including antibodies, cell lines, animals and software tools, with enough information to allow them to be uniquely identified, should be included in the Methods section. Authors are strongly encouraged to cite <a href="#">Research Resource Identifiers</a> (RRIDs) for antibodies, model organisms and tools, where possible.</p> <p>Have you included the information requested as detailed in our <a href="#">Minimum Standards Reporting Checklist</a>?</p>	Yes
<p><b>Availability of data and materials</b></p> <p>All datasets and code on which the conclusions of the paper rely must be either included in your submission or deposited in <a href="#">publicly available repositories</a> (where available and ethically</p>	Yes

appropriate), referencing such data using a unique identifier in the references and in the “Availability of Data and Materials” section of your manuscript.

Have you have met the above requirement as detailed in our [Minimum Standards Reporting Checklist](#)?

1 **Genomic evidence of neo-sex chromosomes in the Eastern Yellow Robin**

2

3 Han Ming Gan<sup>1,2\*</sup>, Stephanie Falk<sup>3</sup>, Hernán E. Morales<sup>4</sup>, Christopher M. Austin<sup>1,2</sup>, Paul  
4 Sunnucks<sup>3</sup>, Alexandra Pavlova<sup>3\*</sup>

5

6 <sup>1</sup> Centre for Integrative Ecology, School of Life and Environmental Sciences, Deakin University,  
7 Geelong, Victoria, Australia

8 <sup>2</sup> Deakin Genomics Centre, Deakin University, Geelong, Victoria, Australia

9 <sup>3</sup> School of Biological Sciences, Monash University, Clayton Campus, Clayton, Victoria, Australia

10 <sup>4</sup> Centre for Marine Evolutionary Biology, Department of Marine Sciences, University of  
11 Gothenburg, Göteborg, Sweden

12

13 **\* Corresponding author:**

14 Name: Han Ming Gan, PhD

15 Address: Building KA4, School of Life and Environmental Sciences, Deakin University,  
16 Waurn Ponds, Victoria 3220, Australia

17 Phone: 0490786277

18 Email: [han.gan@deakin.edu.au](mailto:han.gan@deakin.edu.au)

19

20 Name: Alexandra Pavlova

21 Address: School of Biological Sciences

22 Monash University, Clayton Campus

23 Clayton Victoria 3800

24 Phone: 0399055902

25 Email: [alexandra.pavlova@monash.edu](mailto:alexandra.pavlova@monash.edu)

26

27

28

29

30

31

32

33

34

35 **Abstract**

36

37 **Background:** Understanding sex-biased natural selection can be greatly enhanced by access to  
38 well-annotated chromosomes including ones inherited in sex-specific fashions. The Eastern  
39 Yellow Robin (EYR) is an endemic Australian songbird inferred to have experienced climate-  
40 driven sex-biased selection and is a prominent model for studying mitochondrial-nuclear  
41 interactions in the wild. However, the lack of an EYR reference genome containing both sex  
42 chromosomes (in birds, a female bearing Z and W chromosomes) is limiting current efforts to  
43 understand the mechanisms of these processes. Here, we assemble the genome for a female EYR  
44 and use low depth (10 ×) genome resequencing data from 19 individuals of known sex to identify  
45 chromosome fragments with sex-specific inheritance.

46

47 **Findings:** MaSurCA hybrid assembly using Nanopore and Illumina reads generated a 1.22 Gb  
48 EYR genome in 20,702 scaffolds (94.2% BUSCO completeness). Scaffolds were tested for W-  
49 linked (female-only) inheritance using a *k*-mer approach, and for Z-linked inheritance using  
50 median read-depth test in male and female reads (read-depths must indicate haploid female and  
51 diploid male representation). This resulted in 2,372 W-linked scaffolds (total length: 97,872,282  
52 bp, N<sub>50</sub>: 81,931 bp) and 586 Z-linked scaffolds (total length: 121,817,358 bp, N<sub>50</sub>: 551,641 bp).  
53 Anchoring of the sex-linked EYR scaffolds to the reference genome of a female Zebra Finch  
54 revealed two categories of sex-linked genome region. First, 653 W-linked scaffolds (25.7 Mb)  
55 were anchored to the W sex chromosome and 215 Z-linked scaffolds (74.4 Mb) to the Z. Second,  
56 1138 W-linked scaffolds (70.9 Mb), and 179 Z-linked scaffolds (51.0 Mb), were anchored to a  
57 large section (coordinates ~5 to ~60 Mb) of Zebra Finch chromosome 1A. The first ~5 Mb and last  
58 ~14 Mb of the reference chromosome 1A had only autosomally-behaving EYR scaffolds mapping  
59 to them.

60

61 **Conclusions:** We report a female (W-chromosome containing) EYR genome and provide genomic  
62 evidence for a neo-sex (neo-W and neo-Z) chromosome system in EYR, involving most of a large  
63 chromosome (1A) previously only reported to be autosomal in passerines.

64

65

66 **Keywords:** Eastern Yellow Robin, *Eopsaltria australis*, passerine, songbird, genome, sex  
67 chromosome, W-chromosome, neo-W, neo-Z

68  
69  
70  
71  
72  
73  
74  
75  
76  
77  
78  
79  
80  
81  
82  
83  
84  
85  
86  
87  
88  
89  
90  
91  
92  
93  
94  
95  
96  
97  
98  
99  
100  
101

## Data description

Wildlife species that have genomic variation distributed heterogeneously through environmental and geographic space can be excellent models for studying evolutionary processes under natural conditions. Eastern Yellow Robin (EYR), *Eopsaltria australis*, is a common endemic eastern Australian songbird (Figure 1) that shows geographically discordant patterns of mitochondrial and nuclear genome variation. Whereas nuclear DNA variation in EYR is structured mainly north-to-south, its two mitochondrial lineages (mitolineages) occur in contrasting climates in an east-west (coast-to-inland) direction, with a narrow contact zone between them, despite ongoing male-mediated gene flow [1]. This pattern is inferred to have arisen when EYR experienced two instances of climate-driven mitochondrial introgression into different nuclear backgrounds: from the northern population into the southern through the inland, and from the southern into the northern population along the coast [2]. Because mitogenome divergence is mirrored by a fraction of the EYR nuclear genome that maps to the chromosome 1A of Zebra Finch and is enriched for genes with mitochondrial functions, each inferred mitochondrial introgression is hypothesized to have been accompanied by co-introgression of a co-evolved nuclear region [3]. Accordingly, the species has been highlighted as an exceptional model in the emerging field of ‘mitonuclear ecology’, which addresses evolutionary interactions between mitochondrial and nuclear genomes and their products [4].

Whereas progress on understanding mitonuclear interactions in EYR has been made by mapping genomic reads to a male Zebra Finch *Taeniopygia guttata* reference genome [5], the ~40 million years of evolution between the two species limits the assumptions that can be made about the degree of synteny of their genome organization. Moreover, the male reference lacks the female-specific W chromosome in birds. Nuclear genomic architecture (for example, concentrations of genes with mitochondrial functions that are subject to suppressed recombination), has considerable potential to be a driver of mitonuclear evolution [6]. Furthermore, female-specific selection has been inferred for EYR, based on fine-scale spatial separation of mitolineage distributions and their correlation with climate, despite male-biased gene flow in a species with female-biased dispersal [1]. Accordingly, genomic architecture with the potential to impact the sexes differently could be a key player in mitonuclear evolution in this species. Thus to test among alternative hypotheses concerning mechanisms of potential co-

102 evolution between elements of the nuclear genome and maternally-transmitted mtDNA, reference  
103 sequences of both sex chromosomes are required. For example, the female-specific W-  
104 chromosome is necessarily co-inherited with mitochondrial DNA, and a species could experience  
105 evolution so that W-chromosome bore genes relevant to mitochondrial function [1]. Substantial  
106 female-specific gene regions are known from birds, notably neo-sex chromosome systems that can  
107 provide females with gene sequences unavailable to males [7, 8] .

108 Using a combination of Illumina and Nanopore reads, which have been shown to produce  
109 contiguous genome assemblies [9-12], we assembled a female inland EYR reference genome and  
110 utilized population genomic data from populations harbouring only inland mitochondrial lineages  
111 [13] to identify and annotate W and Z sex chromosomes. This procedure could also detect sex-  
112 linked chromosomes other than the typical W and Z avian sex chromosomes such as neo-sex  
113 chromosomes (caused by fusions between autosomal and sex chromosome elements) that are  
114 uncommon but known in birds, notably throughout the Sylvioidea, and in a honeyeater [7, 8, 14-  
115 16]

116

### 117 **Sample collection, library construction and sequencing**

118

119 Two EYR females, EYR054 and EYR056, were captured at Stuart Mill, western Victoria in the  
120 same net on 6<sup>th</sup> of April 2009, as part of another project [17, 18]. DNA was extracted from 40  $\mu$ L  
121 of blood using a Qiagen DNAeasy Blood and Tissue Kit. A standard paired-end Illumina library  
122 was constructed from 100 ng of QSonica-fragmented (~ 350 bp fragment size) EYR054 DNA  
123 using the NEBUltra Illumina Library Preparation kit (New England Biolabs, Ipswich, MA). The  
124 library was quantified with a TapeStation 4000 (Agilent) and sequenced on the Novaseq6000 (2  $\times$   
125 150 bp run configuration) at the Deakin Genomics Centre. Two Oxford Nanopore sequencing  
126 libraries were constructed from G-tube fragmented (~8 kb) EYR054 gDNA using the LSK108  
127 library preparation kit. Sequencing was performed on two MinION R9.4.1 flowcells for 48 hours  
128 followed by fast5 base-calling using Albacore. A total of 6.63 Gb Nanopore data in 916,218 reads  
129 ( $N_{50}$  = 10,224 bp) were generated after adapter-trimming using Porechop v0.2.3  
130 (<https://github.com/rrwick/Porechop>). Nanopore reads used for this study had 13% error rate,  
131 estimated based on mean pairwise sequence similarity of 87% (median= 89%) between Nanopore  
132 reads and the assembled EYR genome, aligned using Minimap2 [19]. The DNA of EYR056 was  
133 used to construct a mate-pair library with an insert size of 1 kb and sequenced by BGI for earlier  
134 studies [18]. EYR054 is similar genetically to EYR056 according to whole mitogenomes,  
135 microsatellites, and being female contemporaries in an area of the species' range where only the

136 inland mitolineage occurs, in an isolated habitat patch characterized by high local genetic  
137 relatedness [3, 18, 20].

138 For low ( $\sim 10\times$ ) depth whole genome resequencing, 10 female and 9 male EYR individuals  
139 bearing inland mitogenomes (EYR-A) were selected from northern (N=9) and southern (N=10)  
140 populations [2, 13] away from the contact zone between the inland and coastal mitolineages. Prior  
141 to Illumina sequencing, EYR individuals were genetically sexed based on the intron length-  
142 variation of homologous sections of CHD (chromo-helicase-DNA-binding) genes located on W  
143 (female-limited) and Z (occurs in both sexes) chromosomes [21]. These fragments have been  
144 sequenced previously for EYR for both sexes [1]. DNA extraction from 16 blood samples and five  
145 tissues (Supplemental Table 1) was performed using a Qiagen DNAeasy extraction kit. Illumina  
146 library construction and whole genome sequencing were performed at the Deakin Genomics  
147 Centre using the methods described above, generating an average of 17 Gb (min = 12 Gb; max =  
148 31 Gb) sequencing output per sample (Supplemental Table 1).

149

#### 150 **Genome size estimation, hybrid *de novo* assembly and annotation**

151

152 Raw Illumina EYR054 reads were poly-G, adapter- and quality trimmed using fastp v0.18.0 [22].  
153 The trimmed reads were used for genome profiling based on Jellyfish2-calculated *k*-mer frequency  
154 ( $k=25$ ) that estimated a genome size of 993 Mb with 1.12% heterozygosity for EYR054 (Figure  
155 2A) [22-24]. We used MaSuRCA v3.2.4 [25] to perform a hybrid assembly of the EYR054  
156 Nanopore and poly-G trimmed Illumina reads followed by gap-closing with Sealer v2.0.2 [26]. For  
157 the MaSuRCA assembly, Illumina reads were first error-corrected and used to construct contigs  
158 using the de Bruijn graph approach. These contigs were then used to error-correct the Nanopore  
159 long reads generating “mega reads” contigs and used for Overlap-Layout-Consensus assembly.  
160 Subsequently, the MaSuRCA hybrid assembly was gap-closed with Sealer v2.0.2 using Illumina  
161 paired-end reads from the same individual. Given that EYR056 and EYR054 are from the same  
162 population away from the hybrid zone (Harrisson et al. 2012, Morales et al. 2018) and thus likely  
163 possess similar versions of chromosomes, the EYR054 assembly was further scaffolded with mate-  
164 pair data from EYR056 using BESST [27] to generate the final assembly for subsequent analyses  
165 (Table 1). Using mate-pair data improved the assembly  $N_{50}$  from 585 kb to 987 kb. The Sealer-  
166 gap-closed EYR054-only assembly is also made available in the GigaDB , should the future work  
167 on this species require single-individual assembly.

168 BUSCOv3 [28] assessment of the assembled genome based on the avian protein database  
169 (aves\_odb9), indicates 94.2% genome completeness with a low level of duplicated genes (Table



170 1). Prior to gene prediction, the genome was masked for repeats using RepeatModeler v1.0.11 and  
171 RepeatMasker v4.0.7 [29, 30]. The soft-masked genome (15.77% masked, Table 1) along with the  
172 reference proteome of a male Collared Flycatcher [31] were used as the input for BRAKER2  
173 annotation [32], resulting in the prediction of 23,905 genes. The Collared Flycatcher proteome was  
174 used here in preference to Zebra Finch because the former has greater protein similarity to EYR.

175

## 176 **Identification of sex chromosome scaffolds**

177

178 Scaffolds inherited in sex-specific fashions ('sex-linked', 'W-linked' or 'Z-linked') were identified  
179 using two methods (explained below) applied to sequence data obtained from 10 female and 9  
180 male EYR individuals as detailed above. Paired-end reads for each re-sequenced male and female  
181 were poly-G, quality- and adapter-trimmed using fastp (default setting) [22]. The trimmed reads  
182 were mapped to the EYR genome using Bowtie2 v2.3.4 [33]. High mapping rates ranging from  
183 97.82 to 98.53% were observed across all 19 individuals, indicating robust assembly of the female  
184 EYR genome. The read mapping quality reported by Bowtie2 is relatively constant (MapQ >30)  
185 across the assembly albeit with lower quality in the repetitive regions as short reads will not be  
186 able to uniquely map to these regions. Subsequently, 90 million mapped PE reads were  
187 subsampled from each individual (to equalize coverage across individuals) and used to estimate for  
188 each individual the median read-depth for each scaffold, and the fraction of the length of each  
189 scaffold that was covered by reads, using BAMStat04 as implemented in the jvarkit package [34,  
190 35].

191 Genome-wide identification of sex-linked scaffolds based on pooled male and female reads  
192 could be compromised if any individuals had their sexes mis-assigned. Accordingly, to confirm the  
193 sex of the individual to which each set of sequence data was ascribed, the read-depth profiles for  
194 all 19 EYR were assessed for the CHD sexing region noted above. BLASTN was used to align the  
195 CHD-W and CHD-Z nucleotide sequences (GenBank accession KC466840 - KC466844 CHD-W  
196 and KC466845 - KC466853 CHD-Z) to two separate, long scaffolds (W chromosome scaffold:  
197 QKXG01001703.1 - 310,213 bp; Z chromosome scaffold: QKXG01001459.1 - 211,357 bp). For  
198 comparison, an autosomal scaffold, QKXG01002030.1 (3,864,097 bp) was identified that  
199 contained a fragment of the single-copy autosomal GAPDH (glyceraldehyde-3-phosphate  
200 dehydrogenase) gene, sequenced previously for EYR (Genbank accession KC466694- KC466739)  
201 [1]. For the Z chromosome scaffold, a median read-depth centered on  $\sim 5\times$  (haploid depth) was  
202 observed in females, and  $\sim 10\times$  (diploid) in males, while for the W chromosome fragment it was  
203  $\sim 5\times$  (haploid) in females and  $\sim 0\times$  (absent) in males;  $\sim 10\times$  diploid depth was observed for the

204 autosomal scaffold in both sexes (Figure 2B).

205 BAM files from individual EYR were merged by sex using samtools v1.9 [36] to generate  
206 one pooled alignment BAM file per sex. A histogram of read-depth frequency for each sex was  
207 then generated using ‘samtools depth’ to estimate the read-depth cut-off for the identification of  
208 candidate W- and Z-linked scaffolds (Figure 2C). The expected diploid depth for each sex was  
209 estimated based on the peak observed read-depth (male = 77×; female = 83×, Figure 2C). A minor  
210 peak corresponding to haploid read-depth (~40×) was observed for females but not males,  
211 consistent with females being hemizygous for sex-linked regions (Figure 2C). A strong peak of  
212 low read-depth sequences (<5x) was seen only for males, consistent with their lacking a W  
213 chromosome (Figure 2C).

214 To identify candidate W-linked scaffolds, we applied two established approaches with  
215 complementary strengths that take advantage of sequence data being available for each sex. First,  
216 we used a differential mapping approach, based on the expectation that a W-linked scaffold should  
217 exhibit zero median read-depth in males, with a more than 75% of the scaffold having female reads  
218 mapping to it [7, 8]. Second, we used the YGS (‘Y chromosome Genome Scan’) *k*-mer approach,  
219 designed for detecting W- or Y-linked regions [37]. The *k*-mer approach removes identical  
220 repetitive sequences that might lead to false-positive matches to W-linked regions while retaining  
221 useful information from unique variants of repetitive regions: this is an advantageous attribute in  
222 the face of the elevated repetitiveness expected of W chromosome sequences [37]. The *k*-mer  
223 approach was implemented as follows. For the pooled male reads, pooled female reads and the  
224 female EYR genome assembly dataset, separate lists were built of all overlapping 16-bp sequences  
225 (‘16-mers’): *k*=16 was chosen on the basis of genome size, and empirical validation that it  
226 produced bimodal frequency distributions of *k*-mer presences in larger (>1 Gb) genomes [37].  
227 Then, scaffolds from the assembled female genome are assumed to be W-linked if >75% of their  
228 single-copy *k*-mers are absent in the pooled male reads but present in both of the female genome  
229 and pooled female reads.

230 Together, the two approaches identified 2,372 candidate W-linked scaffolds (total length of  
231 97.87 Mb) that were used for downstream analyses. A great majority (1,952, 82.3 %, amounting to  
232 86.32 Mb) of the candidate W-linked scaffolds were identified by both approaches, with 174 (7.3  
233 %, 2.64 Mb) being exclusive to the *k*-mer approach, and 246 (10.4 %, 8.91 Mb) found only by the  
234 differential mapping approach. Inspection of the repetitiveness in the candidate W-linked scaffolds  
235 identified only by the *k*-mer approach indicates that they are 80% repetitive (total repeat  
236 length/total sequence length × 100%), consistent with the high sensitivity of *k*-mer approach in  
237 identifying repetitive sex-linked scaffolds [37]. In contrast, the candidate W-linked scaffolds found

238 by the differential mapping approach alone were only 32.6% repetitive.

239 Since Z-linked scaffolds are present in males and females, it is not possible to utilize the  
240 YGS *k*-mer approach to identify candidates. Thus we identified putative Z-linked scaffolds on the  
241 basis of differences in read-depth between males and females, similar to the differential mapping  
242 method for W-linked scaffold discovery outlined above. To allow for variation in sequencing  
243 depth, we conservatively defined a candidate Z-linked scaffold as one exhibiting more than 58×  
244 median read-depth in males (i.e. 0.75 times the observed male diploid read-depth of 77×) and less  
245 than 62× median read-depth in females (i.e. 1.5 times the observed female haploid read-depth of  
246 41.5×). Scaffolds passing these thresholds were further filtered to retain only those having both  
247 male and female reads mapping to > 75% of the scaffold length. This resulted in the identification  
248 of 586 candidate Z-linked scaffolds with a total length of 121.8 Mb and N<sub>50</sub> of 551.6 kb.

249 The total lengths of W-linked scaffolds (97.87 Mb) and Z-linked scaffolds = 121.82 Mb are  
250 much greater than expected from the typical sizes of sex chromosomes in Passerida, of which EYR  
251 is a member (e.g. in Xu *et al.* 2019 [38], Passerida W chromosomes range from 3.37-4.75 Mb and  
252 Z chromosomes range from 68.8-74.7 Mb) [38]. These observations raised the possibility of the  
253 presence of a neo-sex chromosome system, and hence it was of great interest to compare the sex-  
254 linked regions to a well-annotated reference genome, as follows.

255

### 256 **Genomic evidence of neo-sex chromosomes in Eastern Yellow Robin**

257

258 To assess the accuracy of our approaches for detecting sex-linked regions known in related  
259 reference genomes, and to test for possible neo-sex chromosomes, the candidate W- and Z-linked  
260 scaffolds were separately anchored to the female Zebra Finch genome (bTaeGut2:  
261 [https://vgp.github.io/genomeark/Taeniopygia\\_guttata/](https://vgp.github.io/genomeark/Taeniopygia_guttata/), accessed on 19<sup>th</sup> December 2018) using  
262 RaGoo v1.0 (with default settings) [39]. A total of 215 Z-linked scaffolds (74.4 Mb, ) were  
263 anchored to the Zebra Finch Z chromosome, and 653 W-linked scaffolds (25.7 Mb) to the Zebra  
264 Finch W chromosome. Surprisingly, A substantial proportion of candidate W-linked (n=1138, 70.9  
265 Mb) and Z-linked (n=179, 51.0 Mb) scaffolds were also anchored to the autosomal Zebra Finch  
266 chromosome 1A. Thus, each sex-linked scaffold anchored to one of three female Zebra Finch  
267 chromosomes: W, Z or chromosome 1A. Using the entire EYR draft genome assembly as the  
268 RaGoo input led to the anchoring of several W- and Z-linked scaffolds with the best hits to the  
269 Zebra finch chromosome 1A, resulting in a substantially larger pseudomolecule for chromosome  
270 1A (143.6 Mb), a length that is nearly double that of the Zebra Finch chromosome 1A (71.64 Mb)  
271 which suggests the presence of two separate sex-linked versions of chromosome 1A in EYR (Fig.

272 3). By re-anchoring the EYR scaffolds in the absence of first the candidate W-linked and then the  
273 candidate Z-linked scaffolds, two distinct versions of a chromosome 1A pseudomolecule were  
274 recovered that we designated putative neoZ-1A and neoW-1A chromosomes and used for  
275 subsequent analyses.

276 To assess the robustness of the sex-based scaffold assignment approach, and to check the  
277 sex-specific read-depth and length coverage along the putative neo-sex chromosomes involving  
278 chromosome 1A (which we refer to as “pseudomolecules neoW-1A (Fig. 3 Chr1A: pink bar) and  
279 neoZ-1A (Fig. 3 Chr1A: light blue bar)”), pooled female and male reads were mapped to the  
280 constructed EYR Z, W, autosomal chromosome 5, and neoZ-1A and neoW-1A pseudomolecules.  
281 The mean read-depth in 100 kb non-overlapping sliding windows was calculated using the  
282 ‘coverage’ command in bedtool v2.25.0 [40] and visualized with ggplot2 in R v3.5.2 [41]. The  
283 mean read-depth across the pseudomolecules was largely consistent with the scaffold sex-  
284 assignment i.e. zero depth for males and haploid for females for the W chromosome (Figure 4C)  
285 and neoW-1A (Figure 4A), diploid depth for males and haploid for females for the Z chromosome  
286 (Figure 4D) and neoZ-1A (Figure 4B), and diploid depth for both sexes for autosomal  
287 chromosome 5 (Fig. 4E). In contrast to the W and Z chromosomes, several distinct genomic  
288 regions with read-coverage consistent with that of an autosomal chromosome (Fig 4E) were  
289 observed for neoW-1A (Figure 4A) and neoZ-1A (Figure 4B), mostly at the pseudomolecule  
290 termini.

291

### 292 **Identification of chromosome 1A-anchored gametologous gene pairs**

293 Using FastANI, we calculated the pairwise sequence identity between the neoW-1A or  
294 neoZ-1A pseudomolecule and the Zebra Finch chromosome 1A [42] and found that both exhibited  
295 substantial sequence identity (calculated mean nucleotide identity of 86%) across the whole of  
296 Zebra Finch chromosome 1A (Figure 5A, B). NeoW-1A exhibited ~ 20 Mb greater assembled  
297 length (92.5 Mb) than did neoZ-1A (72.5 Mb) (Figure 5 A, B). Accumulation of repeats  
298 contributed to this: 36.6% of the EYR neoW-1A sequence was characterized as repetitive by  
299 RepeatMasker, while this value is only 10% for the EYR neoZ-1A sequence. Also using FastANI,  
300 we calculated the pairwise sequence identity between EYR neoW-1A and neoZ-1A in a non-  
301 overlapping sliding window of 10 kb. By aligning the putative neoW-1A to the neoZ-A, we  
302 observed high (mostly >90%) pairwise sequence identity throughout the pseudomolecule (Figure  
303 5C). However, there was considerable heterogeneity in absolute sequence similarity, with zones of  
304 ~100 %, ~98 %, ~95 %, and ~92 % identity clumped along the pseudomolecules, suggestive of  
305 evolutionary strata (Figure 5C) [43].

306 Orthologous genes shared between the EYR and Collared Flycatcher (higher protein  
307 similarity to EYR compared to Zebra Finch) were inferred using Orthofinder2 [44]. Of the 957  
308 genes located on the Collared Flycatcher chromosome 1A, 725 formed a one-to-one (N=513) or  
309 one-to-many (N=212) orthologous group with the EYR genes located on the neoZ-1A or neoW-1A  
310 pseudomolecule. We restricted the ortholog analysis to only genes predicted from the sex-linked  
311 scaffolds (identified based on EYR scaffold assignment) since the “autosomal-behaving” scaffolds  
312 on the neoZ-1A and neoW-1A pseudomolecules (Figure 4A and B) may consist of unassigned sex-  
313 linked, recombining sex-linked (collapsed into a single scaffold) or truly autosomal scaffolds that  
314 will affect gametologous pairing. This resulted in the identification of 419 Z-linked genes on EYR  
315 neoZ-1A pseudomolecule and 221 W-linked orthologs on neoW-1A, to a total of 488 different sex-  
316 linked genes. Among these were 148 putative gametologous gene pairs (i.e. homologs with  
317 sufficiently low recombination for one version to be identifiably W- and one Z-linked) between  
318 EYR neoW- and neoZ-1A (Supplemental Table 2). The fewer number of W-linked EYR genes that  
319 formed orthologous group with the Collared Flycatcher chromosome 1A genes compared to that of  
320 Z-linked EYR genes may be due to the more fragmented assembly and higher repetitiveness of W-  
321 linked EYR scaffolds that precludes the accurate annotation of genes in the W-linked scaffolds  
322 when using the default BRAKER2 annotation settings [45]. It is also possible that W-linked EYR  
323 genes on chromosome 1A have diverged, been lost or degraded beyond detection, as expected  
324 under sex chromosome evolution [43].

325 Neo-sex chromosomes have reduced effective population size relative to the autosomes that  
326 contribute to them: this is expected to decreased the effectiveness of purifying selection, especially  
327 when compounded by reduced recombination [46]. These effects should promote the  
328 accumulation of deleterious mutations, commonly revealed as elevated non-synonymous to  
329 synonymous (dN/dS) ratios, particularly for sex-limited chromosomes such as the neo-W in birds  
330 [7, 8, 47]. To calculate the dN/dS ratios for EYR neo-sex gametologous gene pairs, protein  
331 alignment was first performed for all 148 putative neo-sex gametologous gene pairs with their  
332 respective Collared Flycatcher orthologs using Clustal Omega v1.2.1 [48] followed by codon-  
333 based alignment with pal2nal (-nogap option to remove gaps and inframe stop codons) [49]. The  
334 pal2nal output for each orthologous group was used to calculate dN/dS ratios via codeml in paml  
335 v4.9i package [50]. When the Collared Flycatcher orthologous 1A genes were used as the  
336 reference for each comparison, 120 of 148 neoW-1A gametologs exhibited higher dN/dS than their  
337 neoZ-1A gametologous partners (Wilcoxon paired samples signed rank test,  $p = 3.9e-14$ ; Fig. 5 D).

338  
339

## 340 **Conclusion**

341  
342 We report a hybrid genome assembly using Nanopore and Illumina reads of a female Eastern  
343 Yellow Robin (EYR), the first published genome for the family Petroicidae. The identification of  
344 sex-linked scaffolds using a combination of read-depth and *k*-mer YGS approaches followed by  
345 chromosomal anchoring to the genome of a female Zebra Finch, provided strong evidence for the  
346 presence of a neo-sex chromosome system in EYR involving most of chromosome 1A. The  
347 inferred neoW-1A pseudomolecule showed the characteristics expected of a sex-limited neo-sex  
348 chromosome, including elevated dN/dS ratios, increased levels of repetitive sequences and signals  
349 of strata of levels of sequence divergence [7, 8, 47]. Further work is required to understand the  
350 formation of the neo-sex system we infer. One relatively simple model is that one copy of  
351 chromosome 1A fused with the W chromosome, and the second copy of chromosome 1A became  
352 inherited in a neo-Z fashion; but more complicated scenarios are possible [7, 8, 15]. Given that the  
353 divergence between inland and coastal EYR lineages is partly due to a genomic region enriched for  
354 nuclear genes with mitochondrial functions that maps to the autosomal chromosome 1A in other  
355 songbirds [3](Morales et al. 2018), the role of neo-sex chromosomes in maintaining lineage  
356 divergence despite nuclear gene flow warrants further investigation involving a female genome of  
357 the coastal lineage. Future work should also test whether unlikely but possible neoZ-1A difference  
358 between the EYR054 used for assembly here and EYR056 used for scaffolding affected the neo-Z  
359 assembly. Chromosome 1A is not one of the chromosomes implicated in multiple known  
360 vertebrate neo-sex systems [47], but given its unusual concentration of genes with mitochondrial  
361 functions, it will not be surprising if subsequent equivalent cases are found [3]. Our results show  
362 that assuming close synteny between a songbird of interest and a distantly-related reference  
363 genome can lead to incomplete or incorrect evolutionary inferences. The present genome assembly  
364 will be an important molecular resource for understanding and re-evaluating genome evolution in  
365 EYR, a key model wildlife species in the emerging field of ‘mitonuclear ecology’ [4]. The  
366 discovery of neo-sex chromosomes in this bird species adds another, independent model to the  
367 limited number in which sex chromosome evolution can be studied through the lens of relatively  
368 young sex chromosomes [15, 47].

369

370

371

372

373 **Availability of supporting data**

374 The genome assembly has been deposited in the NCBI database with the accession number  
375 QKXG010000000. Raw sequencing data have been deposited in the NCBI Sequence Read Archive  
376 (SRA) database and linked to the Bioproject ID PRJNA476023.

377

378 **Competing interests**

379 The authors declare that they have no competing interests.

380

381 **Funding**

382 This study was funded by the Monash School of Biological Sciences, Australian Research Council  
383 (ARC) Discovery Project (DP180102359), ARC Linkage Grant (LP0776322), the Victorian  
384 Department of Sustainability and Environment (DSE), Museum of Victoria, Victorian Department  
385 of Primary Industries, Parks Victoria, North Central Catchment Management Authority, Goulburn  
386 Broken Catchment Management Authority, CSIRO Ecosystem Sciences, and the Australian  
387 National Wildlife Collection Foundation.

388

389 **Authors' contributions**

390 HMG, PS and AP conceived the study. HEM and SF collected the samples and extracted the  
391 genomic DNA. CMA contributed sequencing reagents and computing resources. HMG performed  
392 whole-genome sequencing, genome assembly, genome annotation and comparative genomics  
393 analysis. HEM assessed the assembly quality and genomics analysis. HMG, AP and PS wrote the  
394 manuscript. All authors read, edited and approved the final manuscript.

395

396 **Acknowledgments**

397 We thank Nevil Amos, Lana Austin and all other collectors of specimens and all agencies who  
398 granted permission to collect specimens. Field samples were collected under scientific research  
399 permits issued by the Victorian Department of Environment and Primary Industries (numbers  
400 10007165, 10005919 and 10005514), New South Wales Office of Environment and Heritage  
401 (SL100886), in accordance with Animal Ethics approvals AM13-05, BSCI\_2012\_20 and  
402 BSCI\_2007\_07, using bands issued by the Australian Bird and Bat Banding Scheme. We also  
403 thank the Australian National Wildlife Collection, Leo Joseph, Robert Palmer and Richard Major  
404 for providing genetic samples. We are grateful to Erich Jarvis and Olivier Fedrigo for giving us  
405 access to the female Zebra Finch assembly. We thank Gabriel Low for helpful discussion.

406

407 **Figure legends**

408

409 Figure 1. The Eastern Yellow Robin. Photo by Geoff Park

410

411 Figure 2. Genomic profiling and *in-silico* sexing of Eastern Yellow Robin. (A) Genomescope  
412 profile calculated from trimmed Illumina data of EYR054 using a *k*-mer length of 25. (B) Median  
413 coverage per individual for three sets of scaffolds with different inheritance, for the female sample  
414 (N=10) and male sample (N=9), with individuals sequenced at ~ 10x coverage each. Autosomal =  
415 GAPDH-containing chromosome fragment [1] scaffold QKXG0002030; W = W-chromosome  
416 fragment: scaffold QKXG0001703; Z = Z chromosome fragment: scaffold QKXG0001459. (C)  
417 Frequency distribution of base-by-base read-depth calculated from the mapping of pooled male  
418 (blue line) and female (red line) reads to the female genome assembly. This is subsequently used to  
419 estimate the read-depth of haploid and diploid scaffolds.

420

421 Figure 3. The assembled lengths of Eastern Yellow Robin (EYR) chromosome 1A, W and Z  
422 pseudomolecules constructed by anchoring different scaffold inputs to the female Zebra Finch  
423 reference genome (ZF; grey bars). Inputs included: EYR genome (EYR; yellow bars); EYR  
424 candidate W-linked scaffolds (EYR W-linked; red bars); EYR candidate Z-linked scaffolds (EYR  
425 Z-linked; dark blue bars); EYR genome without Z-linked scaffolds (EYR w/o Z-linked; pink bars);  
426 EYR genome without W-linked scaffolds (EYR w/o W-linked; light blue bars). Neo-sex-  
427 chromosome pseudomolecules were built using the latter two datasets (the length of neoW-1A is  
428 shown by the light blue bar and that of neoZ-1A by the light pink bar for Ch1A).

429

430 Figure 4. Read-depth of pooled male (blue dots) and pooled female (red dots) reads across EYR  
431 pseudomolecules neoW-1A, neoZ-1A, W, Z and autosomal chromosome 5. Read-depth (the  
432 number of reads for each nucleotide in the genome) was estimated for each 100 kb sliding window.  
433 The locations of candidate W-linked scaffolds on the neoW-1A and Z-linked scaffolds on neoZ-1A  
434 pseudomolecules are indicated by the black lines below the read-depth plots. Coordinate (Mb)  
435 refers to the position on the pseudomolecule.

436

437 Figure 5. Characterization of the inferred neo-sex chromosomes in Eastern Yellow Robin. Linear  
438 genome comparison of the (A) neoW-1A and (B) neoZ-1A pseudomolecules (blue horizontal bars)  
439 with the Zebra Finch chromosome 1A (green horizontal bars). The neoW-1A alignment is ~ 20 Mb  
440 longer than that of neoZ-1A. The red lines denote regions of nucleotide similarity with more than



441 70% nucleotide identity calculated over 10 kb non-overlapping sliding window. (C) Pairwise  
 442 sequence identity per 10 kb sliding window (to obtain high resolution) between the neoW-1A and  
 443 neoZ-1A scaffolds mapped along the neoZ-1A pseudomolecule, with coordinates relating to the  
 444 neoZ-1A pseudomolecule. Zones of different levels of sequence similarity can be seen along the  
 445 pseudomolecule. The blue line denotes the smoothed conditional means for pairwise identity and  
 446 the grey zone around it indicates the 95% confidence interval. (D) Paired box plots showing the  
 447 dN/dS ratios of neoW-1A and neoZ-1A gene copies (gametologs) of the Eastern Yellow Robin  
 448 compared with Collared Flycatcher orthologs as references. Collared Flycatcher was used here in  
 449 preference to Zebra Finch because the former has greater protein similarity to EYR. Grey lines  
 450 connecting red and blue dots represent gametologs.

451  
 452

453 **Table 1**

454 Table 1. Genome assembly and annotation statistics of the Eastern Yellow Robin

Parameter	Details
Organism	<i>Eopsaltria australis</i> (Eastern Yellow Robin)
Isolate	EYR054 (sex = female; data type: Illumina standard paired-end and Nanopore long read)  EYR056 (sex = female; data type: Illumina mate-pair)
Bioproject	PRJNA476023
Biosample	SAMN09425179 (isolate EYR054)  SAMN10581952 (isolate EYR056)
GenBank assembly accession	GCA_003426825.1 (QKXG01)
Assembled Length	1,228,344,903 bp
Scaffold N <sub>50</sub>	987,278 bp
Number of scaffolds	20,702
Number of predicted genes	23,905

### **Repeat Annotation:**

LINES	39,888,415 bp (3.25%)
LTR elements	85,519,635 (6.96%)
DNA elements	6,416,492 (0.52%)
Unclassified repeats	42,749,317 (3.48%)
Satellites	1,967,923 (0.16%)
Simple repeats	14,300,770 (1.16%)
Low complexity	3,128,912 (0.25%)

<b><u>BUSCO completeness (Ave odb9)</u></b>	<b><u>Whole genome</u></b>	<b><u>Predicted proteome</u></b>
Complete BUSCO	4,627 (94.2%)	3,795 (77.2%)
Complete and single-copy BUSCO	4,436 (90.3%)	3,302 (67.2%)
Complete and duplicated BUSCO	191 (3.9%)	493 (10.0%)
Fragmented BUSCO	163 (3.3%)	590 (12.0%)
Missing BUSCO	125 (2.5%)	530 (10.8%)
Total BUSCO groups search	4,915	4,915

---

455

456

### 457 **References**

458

- 459 1. Pavlova A, Amos JN, Joseph L, Loynes K, Austin JJ, Keogh JS, et al. Perched at the mito-nuclear  
460 crossroads: divergent mitochondrial lineages correlate with environment in the face of ongoing  
461 nuclear gene flow in an Australian bird. *Evolution*. 2013;67 12:3412-28.
- 462 2. Morales HE, Sunnucks P, Joseph L and Pavlova A. Perpendicular axes of differentiation generated  
463 by mitochondrial introgression. *Molecular ecology*. 2017;26 12:3241-55.
- 464 3. Morales HE, Pavlova A, Amos N, Major R, Kilian A, Greening C, et al. Concordant divergence of  
465 mitogenomes and a mitonuclear gene cluster in bird lineages inhabiting different climates. *Nature*  
466 *ecology & evolution*. 2018;2 8:1258.
- 467 4. Hill GE. *Mitonuclear ecology*. Oxford, United Kingdom: Oxford University Press; 2019.
- 468 5. Warren WC, Clayton DF, Ellegren H, Arnold AP, Hillier LW, Künstner A, et al. The genome of a  
469 songbird. *Nature*. 2010;464:757. doi:10.1038/nature08819

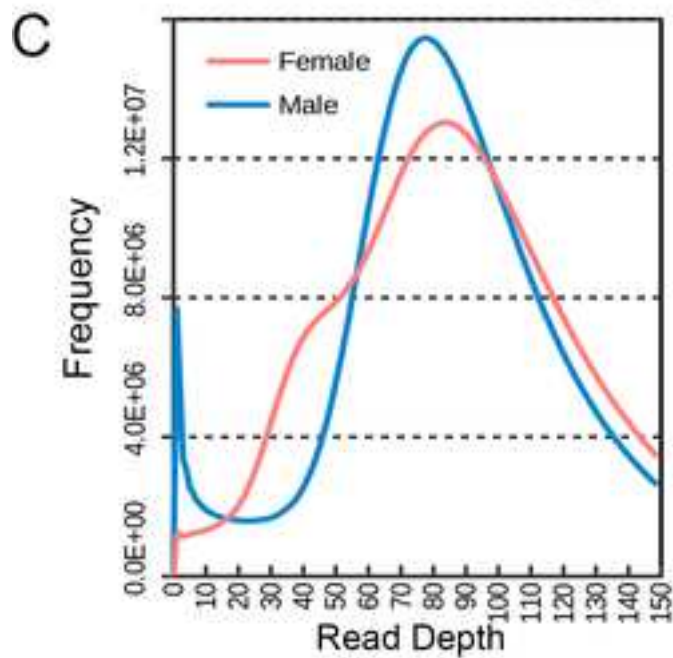
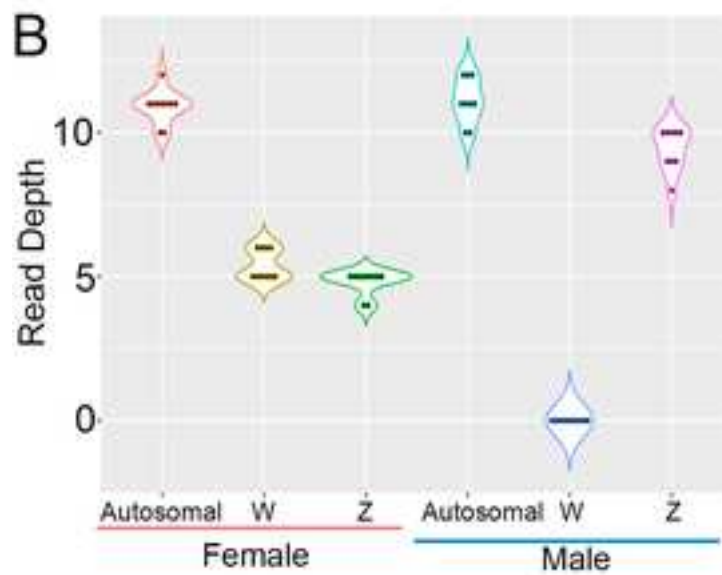
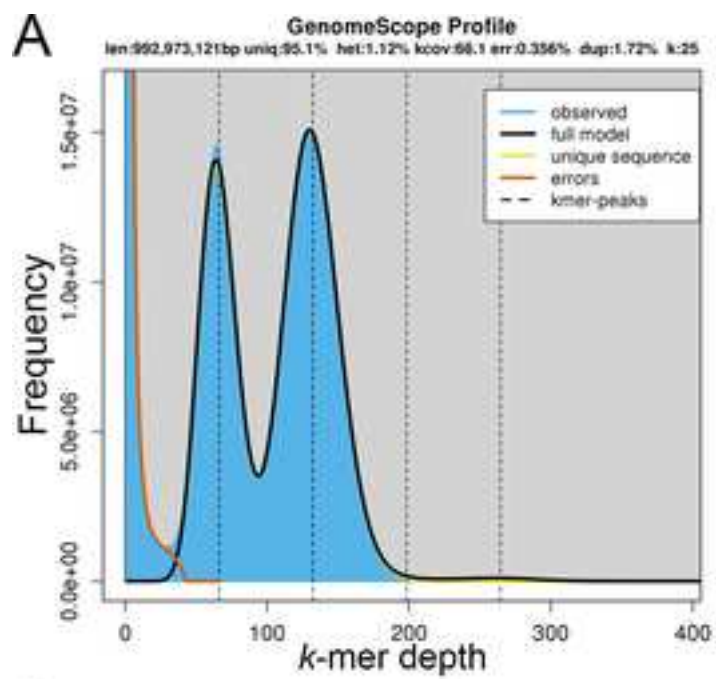
- 470 <https://www.nature.com/articles/nature08819#supplementary-information>.
- 471 6. Sunnucks P, Morales HE, Lamb AM, Pavlova A and Greening C. Integrative approaches for studying  
472 mitochondrial and nuclear genome co-evolution in oxidative phosphorylation. *Frontiers in*  
473 *genetics*. 2017;8:25.
- 474 7. Dierickx E, Sin S, van Veelen P, Brooke MdL, Liu Y, Edwards S, et al. Neo-sex chromosomes and  
475 demography shape genetic diversity in the Critically Endangered Raso lark. *bioRxiv*. 2019:617563.  
476 doi:10.1101/617563.
- 477 8. Leroy T, Anselmetti Y, Tilak M-K, Bérard S, Csukonyi L, Gabrielli M, et al. A bird's white-eye view on  
478 neosex chromosome evolution. *bioRxiv*. 2019:505610. doi:10.1101/505610.
- 479 9. Austin CM, Tan MH, Harrisson KA, Lee YP, Croft LJ, Sunnucks P, et al. De novo genome assembly  
480 and annotation of Australia's largest freshwater fish, the Murray cod (*Maccullochella peelii*), from  
481 Illumina and Nanopore sequencing read. *Gigascience*. 2017;6 8:1-6.
- 482 10. Tan MH, Austin CM, Hammer MP, Lee YP, Croft LJ and Gan HM. Finding Nemo: hybrid assembly  
483 with Oxford Nanopore and Illumina reads greatly improves the clownfish (*Amphiprion ocellaris*)  
484 genome assembly. *GigaScience*. 2018;7 3:gix137.
- 485 11. Zimin AV, Puiu D, Luo M-C, Zhu T, Koren S, Marçais G, et al. Hybrid assembly of the large and  
486 highly repetitive genome of *Aegilops tauschii*, a progenitor of bread wheat, with the MaSuRCA  
487 mega-reads algorithm. *Genome research*. 2017.
- 488 12. Zimin AV, Puiu D, Hall R, Kingan S, Clavijo BJ and Salzberg SL. The first near-complete assembly of  
489 the hexaploid bread wheat genome, *Triticum aestivum*. *Gigascience*. 2017;6 11:1-7.  
490 doi:10.1093/gigascience/gix097.
- 491 13. Morales HE, Pavlova A, Joseph L and Sunnucks P. Positive and purifying selection in mitochondrial  
492 genomes of a bird with mitonuclear discordance. *Mol Ecol*. 2015;24 11:2820-37.  
493 doi:10.1111/mec.13203.
- 494 14. Sardell J. *Evolutionary Consequences of Recent Secondary Contact Between Myzomela*  
495 *Honeyeaters*. 2016.
- 496 15. Pala I, Naurin S, Stervander M, Hasselquist D, Bensch S and Hansson B. Evidence of a neo-sex  
497 chromosome in birds. *Heredity (Edinb)*. 2012;108 3:264-72. doi:10.1038/hdy.2011.70.
- 498 16. Brooke Mde L, Welbergen JA, Mainwaring MC, van der Velde M, Harts AM, Komdeur J, et al.  
499 Widespread translocation from autosomes to sex chromosomes preserves genetic variability in an  
500 endangered lark. *Journal of molecular evolution*. 2010;70 3:242-6. doi:10.1007/s00239-010-9333-  
501 3.
- 502 17. Harrisson KA, Pavlova A, Amos JN, Takeuchi N, Lill A, Radford JQ, et al. Fine-scale effects of habitat  
503 loss and fragmentation despite large-scale gene flow for some regionally declining woodland bird  
504 species. *Landscape Ecology*. 2012;27 6:813-27. doi:10.1007/s10980-012-9743-2.
- 505 18. Morales HE, Pavlova A, Sunnucks P, Major R, Amos N, Joseph L, et al. Neutral and selective drivers  
506 of colour evolution in a widespread Australian passerine. *Journal of biogeography*. 2017;44 3:522-  
507 36.
- 508 19. Li H. Minimap2: pairwise alignment for nucleotide sequences. *Bioinformatics*. 2018;34 18:3094-  
509 100. doi:10.1093/bioinformatics/bty191.
- 510 20. Amos JN, Harrisson KA, Radford JQ, White M, Newell G, Nally RM, et al. Species- and sex-specific  
511 connectivity effects of habitat fragmentation in a suite of woodland birds. *Ecology*. 2014;95  
512 6:1556-68. doi:10.1890/13-1328.1.
- 513 21. Griffiths R, Double MC, Orr K and Dawson RJ. A DNA test to sex most birds. *Molecular ecology*.  
514 1998;7 8:1071-5.
- 515 22. Chen S, Zhou Y, Chen Y and Gu J. fastp: an ultra-fast all-in-one FASTQ preprocessor.  
516 *Bioinformatics*. 2018;34 17:i884-i90. doi:10.1093/bioinformatics/bty560.
- 517 23. Marçais G and Kingsford C. A fast, lock-free approach for efficient parallel counting of occurrences  
518 of k-mers. *Bioinformatics*. 2011;27 6:764-70. doi:10.1093/bioinformatics/btr011.
- 519 24. Vurture GW, Sedlazeck FJ, Nattestad M, Underwood CJ, Fang H, Gurtowski J, et al. GenomeScope:  
520 fast reference-free genome profiling from short reads. *Bioinformatics*. 2017;33 14:2202-4.

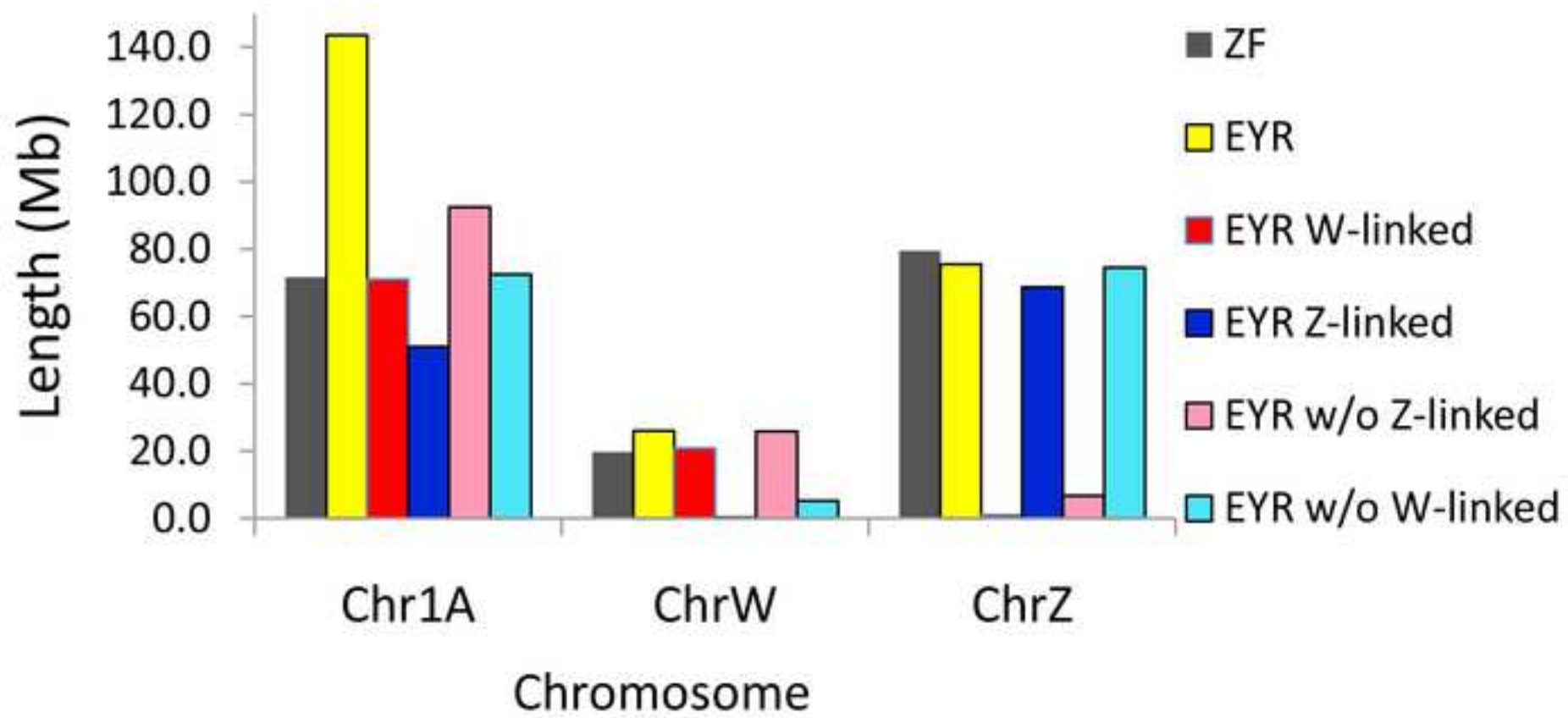
- 521 25. Zimin AV, Marçais G, Puiu D, Roberts M, Salzberg SL and Yorke JA. The MaSuRCA genome  
522 assembler. *Bioinformatics*. 2013;29 21:2669-77.
- 523 26. Paulino D, Warren RL, Vandervalk BP, Raymond A, Jackman SD and Birol I. Sealer: a scalable gap-  
524 closing application for finishing draft genomes. *BMC bioinformatics*. 2015;16 1:230.
- 525 27. Sahlin K, Chikhi R and Arvestad L. Assembly scaffolding with PE-contaminated mate-pair libraries.  
526 *Bioinformatics*. 2016;32 13:1925-32.
- 527 28. Waterhouse RM, Seppey M, Simão FA, Manni M, Ioannidis P, Klioutchnikov G, et al. BUSCO  
528 applications from quality assessments to gene prediction and phylogenomics. *Molecular biology  
529 and evolution*. 2017;35 3:543-8.
- 530 29. Smit AF, Hubley R and Green P. RepeatMasker. 1996.
- 531 30. Smit A and Hubley R. RepeatModeler Open-1.0. Available from [http://www](http://www.repeatmasker.org)  
532 repeatmasker.org. 2008.
- 533 31. Ellegren H, Smeds L, Burri R, Olason PI, Backström N, Kawakami T, et al. The genomic landscape of  
534 species divergence in *Ficedula* flycatchers. *Nature*. 2012;491 7426:756.
- 535 32. Hoff KJ, Lange S, Lomsadze A, Borodovsky M and Stanke M. BRAKER1: unsupervised RNA-Seq-  
536 based genome annotation with GeneMark-ET and AUGUSTUS. *Bioinformatics*. 2015;32 5:767-9.
- 537 33. Langmead B and Salzberg SL. Fast gapped-read alignment with Bowtie 2. *Nature methods*. 2012;9  
538 4:357.
- 539 34. Lindenbaum P. Jvarkit: java-based utilities for Bioinformatics. 2015.
- 540 35. Lindenbaum P and Redon R. bioalcaide, samjs and vcfilterjs: object-oriented formatters and filters  
541 for bioinformatics files. *Bioinformatics*. 2018;34 7:1224-5. doi:10.1093/bioinformatics/btx734.
- 542 36. Li H, Handsaker B, Wysoker A, Fennell T, Ruan J, Homer N, et al. The Sequence Alignment/Map  
543 format and SAMtools. *Bioinformatics*. 2009;25 16:2078-9. doi:10.1093/bioinformatics/btp352.
- 544 37. Carvalho AB and Clark AG. Efficient identification of Y chromosome sequences in the human and  
545 *Drosophila* genomes. *Genome research*. 2013;23 11:1894-907. doi:10.1101/gr.156034.113.
- 546 38. Xu L, Auer G, Peona V, Suh A, Deng Y, Feng S, et al. Dynamic evolutionary history and gene content  
547 of sex chromosomes across diverse songbirds. *Nat Ecol Evol*. 2019;3 5:834-44.  
548 doi:10.1038/s41559-019-0850-1.
- 549 39. Alonge M, Soyk S, Ramakrishnan S, Wang X, Goodwin S, Sedlazeck FJ, et al. Fast and accurate  
550 reference-guided scaffolding of draft genomes. *bioRxiv*. 2019:519637. doi:10.1101/519637.
- 551 40. Quinlan AR and Hall IM. BEDTools: a flexible suite of utilities for comparing genomic features.  
552 *Bioinformatics*. 2010;26 6:841-2. doi:10.1093/bioinformatics/btq033.
- 553 41. Wickham H. ggplot2: Elegant Graphics for Data Analysis. Springer Publishing Company,  
554 Incorporated; 2009.
- 555 42. Jain C, Rodriguez-R LM, Phillippy AM, Konstantinidis KT and Aluru S. High throughput ANI analysis  
556 of 90K prokaryotic genomes reveals clear species boundaries. *Nature communications*. 2018;9  
557 1:5114.
- 558 43. Wright AE, Dean R, Zimmer F and Mank JE. How to make a sex chromosome. *Nature  
559 communications*. 2016;7:12087.
- 560 44. Emms DM and Kelly S. OrthoFinder: solving fundamental biases in whole genome comparisons  
561 dramatically improves orthogroup inference accuracy. *Genome biology*. 2015;16 1:157.
- 562 45. Rutkowska J, Lagisz M and Nakagawa S. The long and the short of avian W chromosomes: no  
563 evidence for gradual W shortening. *Biology letters*. 2012;8 4:636-8. doi:10.1098/rsbl.2012.0083.
- 564 46. Smeds L, Warmuth V, Bolivar P, Uebbing S, Burri R, Suh A, et al. Evolutionary analysis of the  
565 female-specific avian W chromosome. *Nature communications*. 2015;6:7330.
- 566 47. Sigeman H, Ponnikas S, Videvall E, Zhang H, Chauhan P, Naurin S, et al. Insights into Avian  
567 Incomplete Dosage Compensation: Sex-Biased Gene Expression Coevolves with Sex Chromosome  
568 Degeneration in the Common Whitethroat. *Genes*. 2018;9 8 doi:10.3390/genes9080373.
- 569 48. Sievers F and Higgins DG. Clustal Omega, accurate alignment of very large numbers of sequences.  
570 *Multiple sequence alignment methods*. Springer; 2014. p. 105-16.

- 571 49. Suyama M, Torrents D and Bork P. PAL2NAL: robust conversion of protein sequence alignments  
572 into the corresponding codon alignments. *Nucleic acids research*. 2006;34 suppl\_2:W609-W12.  
573 50. Yang Z. PAML 4: phylogenetic analysis by maximum likelihood. *Molecular biology and evolution*.  
574 2007;24 8:1586-91.
- 575

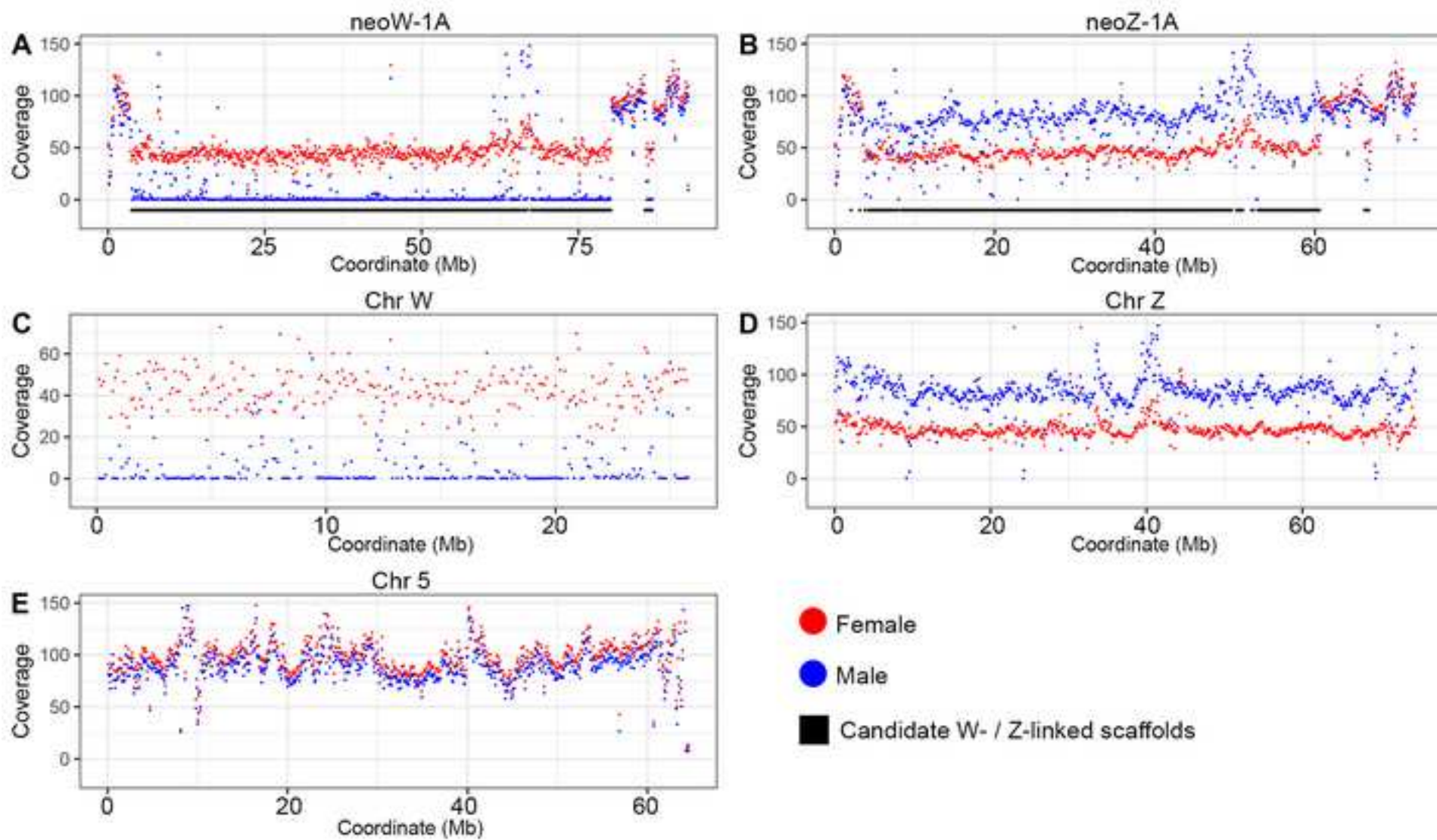


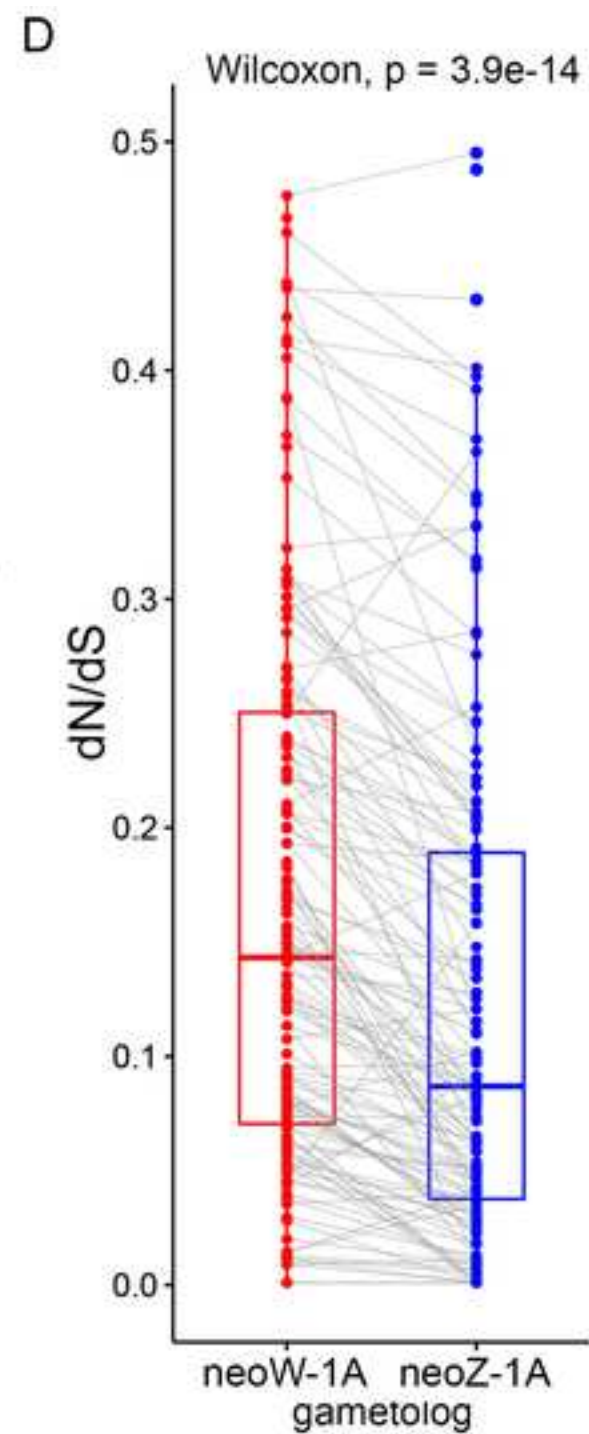
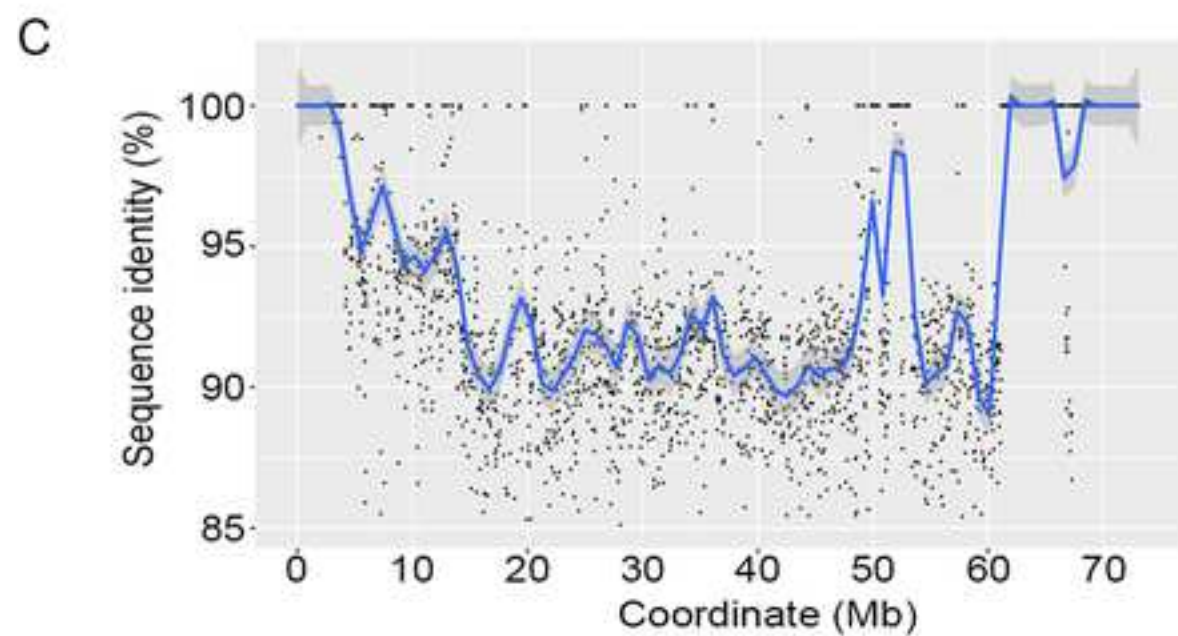
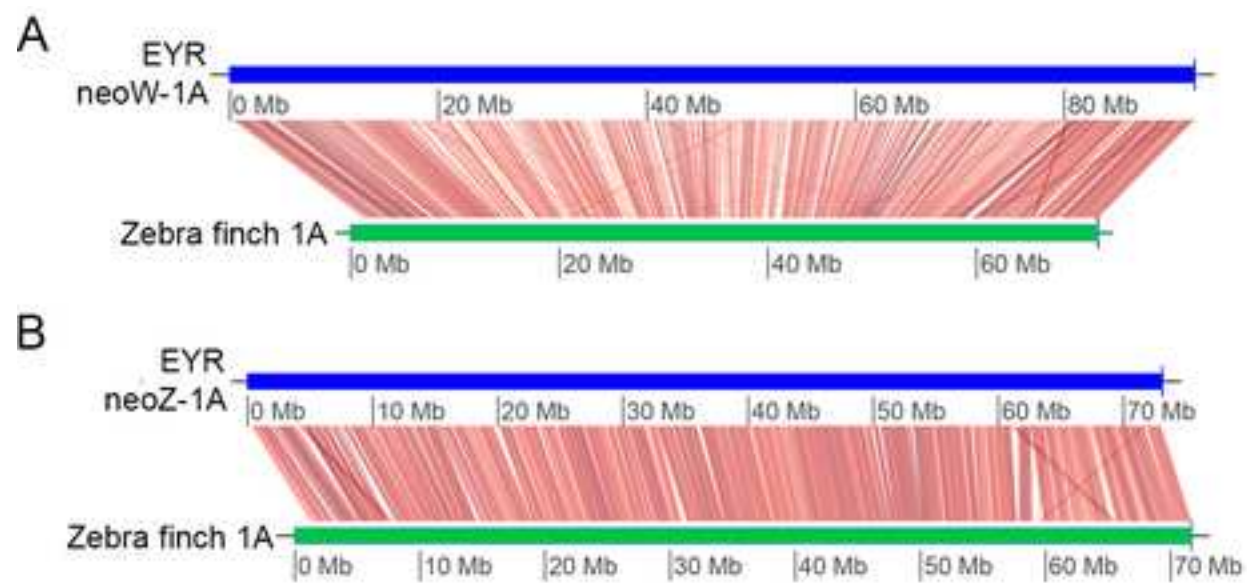


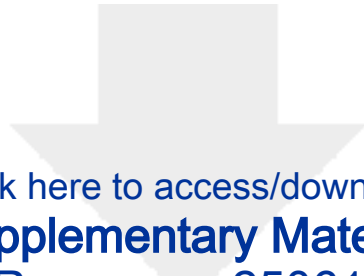












Click here to access/download  
**Supplementary Material**  
EYR\_Response\_250619.docx







Click here to access/download  
**Supplementary Material**  
SupplementalTable2.xls